



# NAVAL POSTGRADUATE SCHOOL

MONTEREY, CALIFORNIA

## THESIS

### CONTROL OF A SYSTEM IN THE PRESENCE OF FLEXIBLE MODES

by

Eleftherios Manos

June 2007

Thesis Advisor:  
Second Reader:

Roberto Cristi  
Xiaoping Yun

**Approved for public release; distribution is unlimited**

THIS PAGE INTENTIONALLY LEFT BLANK

<b>REPORT DOCUMENTATION PAGE</b>			<i>Form Approved OMB No. 0704-0188</i>	
Public reporting burden for this collection of information is estimated to average 1 hour per response, including the time for reviewing instruction, searching existing data sources, gathering and maintaining the data needed, and completing and reviewing the collection of information. Send comments regarding this burden estimate or any other aspect of this collection of information, including suggestions for reducing this burden, to Washington headquarters Services, Directorate for Information Operations and Reports, 1215 Jefferson Davis Highway, Suite 1204, Arlington, VA 22202-4302, and to the Office of Management and Budget, Paperwork Reduction Project (0704-0188) Washington DC 20503.				
<b>1. AGENCY USE ONLY (Leave blank)</b>		<b>2. REPORT DATE</b> June 2007	<b>3. REPORT TYPE AND DATES COVERED</b> Master's Thesis	
<b>4. TITLE AND SUBTITLE:</b> Control of a System in the Presence of Flexible Modes			<b>5. FUNDING NUMBERS</b>	
<b>6. AUTHOR(S)</b> Eleftherios Manos				
<b>7. PERFORMING ORGANIZATION NAME(S) AND ADDRESS(ES)</b> Naval Postgraduate School Monterey, CA 93943-5000			<b>8. PERFORMING ORGANIZATION REPORT NUMBER</b>	
<b>9. SPONSORING /MONITORING AGENCY NAME(S) AND ADDRESS(ES)</b> N/A			<b>10. SPONSORING/MONITORING AGENCY REPORT NUMBER</b>	
<b>11. SUPPLEMENTARY NOTES</b> The views expressed in this thesis are those of the author and do not reflect the official policy or position of the Department of Defense or the U.S. Government.				
<b>12a. DISTRIBUTION / AVAILABILITY STATEMENT</b> Approved for public release; distribution is unlimited			<b>12b. DISTRIBUTION CODE</b>	
<b>13. ABSTRACT (maximum 200 words)</b>  The primary research objective is to investigate the control of flexible space structures—mobile satellite communication systems in particular. Solar-powered satellites require a high level of accuracy in attitude stabilization and large-angle maneuvering. Furthermore, they have to be least sensitive to disturbances affecting the structure, possibly coming from several sources, such as mechanical vibrations due to flexible panels appended to the spacecraft. In this thesis, we address the problem of robust adaptive disturbance rejection in a control system of a flexible structure. The intent is to guarantee stability and maximum rejection of the disturbances. For the achievement of this purpose, a Linear Quadratic Gaussian (LQG) controller is designed using Loop Transfer Recovery (LTR) in order to increase the robustness of the system. A second approach is to design a nonminimum-phase structural filter and to examine its effect on the system's stability.				
<b>14. SUBJECT TERMS</b> State Space Analysis, Linear Quadratic Gaussian Controller, Loop Transfer Recovery Approach			<b>15. NUMBER OF PAGES</b> 65	
			<b>16. PRICE CODE</b>	
<b>17. SECURITY CLASSIFICATION OF REPORT</b> Unclassified	<b>18. SECURITY CLASSIFICATION OF THIS PAGE</b> Unclassified	<b>19. SECURITY CLASSIFICATION OF ABSTRACT</b> Unclassified	<b>20. LIMITATION OF ABSTRACT</b> UL	

NSN 7540-01-280-5500

Standard Form 298 (Rev. 2-89)  
Prescribed by ANSI Std. Z39-18

THIS PAGE INTENTIONALLY LEFT BLANK

**Approved for public release; distribution is unlimited**

**CONTROL OF A SYSTEM IN THE PRESENCE OF FLEXIBLE MODES**

Eleftherios Manos  
Lieutenant Junior Grade, Hellenic Navy  
B.S., Hellenic Naval Academy, 2000

Submitted in partial fulfillment of the  
requirements for the degree of

**MASTER OF SCIENCE IN ELECTRICAL ENGINEERING**

from the

**NAVAL POSTGRADUATE SCHOOL  
June 2007**

Author: Eleftherios Manos

Approved by: Roberto Cristi  
Thesis Advisor

Xiaoping Yun  
Second Reader

Jeffrey B. Knorr  
Chairman, Department of Electrical and Computer Engineering

THIS PAGE INTENTIONALLY LEFT BLANK

## **ABSTRACT**

The primary research objective is to investigate the control of flexible space structures—mobile satellite communication systems in particular. Solar-powered satellites require a high level of accuracy in attitude stabilization and large-angle maneuvering. Furthermore, they have to be least sensitive to disturbances affecting the structure, possibly coming from several sources, such as mechanical vibrations due to flexible panels appended to the spacecraft. In this thesis, we address the problem of robust adaptive disturbance rejection in a control system of a flexible structure. The intent is to guarantee stability and maximum rejection of the disturbances. For the achievement of this purpose, a Linear Quadratic Gaussian (LQG) controller is designed using Loop Transfer Recovery (LTR) in order to increase the robustness of the system. A second approach is to design a nonminimum-phase structural filter and to examine its effect on the system's stability.

THIS PAGE INTENTIONALLY LEFT BLANK

## TABLE OF CONTENTS

I.	INTRODUCTION.....	1
II.	MODELING FOR CONTROL OF FLEXIBLE STRUCTURES .....	5
A.	FLEXIBLE STRUCTURE.....	5
B.	STATE SPACE MODELING.....	7
III.	STATE FEEDBACK / LINEAR QUADRATIC REGULATOR .....	11
A.	STABILITY.....	11
B.	OPTIMIZATION / LINEAR QUADRATIC (LQR) REGULATOR .....	11
C.	ROBUSTNESS / STABILITY OF LQR DESIGN.....	14
IV.	LINEAR QUADRATIC GAUSSIAN / LOOP TRANSFER RECOVERY DESIGN (LQG/LTR) .....	19
A.	LINEAR QUADRATIC GAUSSIAN (LQG) .....	19
B.	LOOP TRANSFER RECOVERY .....	24
V.	STRUCTURAL FILTER DESIGN.....	33
A.	NON MINIMUM PHASE STRUCTURE FILTER.....	33
B.	COMPARISON OF THE LQG/LTR AND NONMINIMUM PHASE NOTCH FILTER DESIGNS .....	38
VI.	CONCLUSIONS AND RECOMMENDATIONS.....	43
	LIST OF REFERENCES .....	45
	INITIAL DISTRIBUTION LIST .....	47

THIS PAGE INTENTIONALLY LEFT BLANK

## LIST OF FIGURES

Figure 1.	Pole-zero map of a flexible mode. ....	7
Figure 2.	State Space Model. [Hespanha]. ....	7
Figure 3.	Model representation. ....	9
Figure 4.	Linear Quadratic Regulator Block Diagram. ....	12
Figure 5.	Bode plot of OPLTF of the LQR design in the nominal frequency. ....	13
Figure 6.	Impulse Response of the LQR CLTF. ....	14
Figure 7.	Bode plot of OPLTF in the presence of -5% to 5% increment of the nominal frequency. ....	15
Figure 8.	Bode plot of OPLTF in the presence of -10% to 10% increment of the nominal frequency. ....	16
Figure 9.	Bode plot of OPLTF in the presence of -20% to 20% increment of the nominal frequency. ....	17
Figure 10.	Linear Quadratic Gaussian Block Diagram. ....	20
Figure 11.	Impulse response of the LQG CLTF. ....	21
Figure 12.	Bode plot of OPLTF of the LQG design. ....	22
Figure 13.	Impulse response of the CLTF of the LQG design in the presence of 5% increment in the frequency of the flexible mode. ....	23
Figure 14.	Bode plot of the OPLTF of the LQG design in the presence of 5% increment of the flexible mode frequency. ....	24
Figure 15.	Bode plots of OPLTF of the LQR and the LQG/LTR controllers for $g=10$ . ...	27
Figure 16.	Bode plots of OPLTF of the LQR and the LQG/LTR controllers for $g=100$ . ....	28
Figure 17.	Bode plots of OPLTF of the LQR and the LQG/LTR controllers for $g=1000$ . ....	29
Figure 18.	Bode plots of OPLTF of the LQR and the LQG/LTR controllers for $g=10,000$ . ....	30
Figure 19.	Nyquist plot of the OPLTF at the nominal frequency for several values of $g$ . ....	31
Figure 20.	Nyquist plot of the OPLTF at the presence of 10% increment of the nominal frequency for several values of $g$ . ....	32
Figure 21.	Pole-Zero map of the OPLTF of the two-mass-spring example. ....	33
Figure 22.	Two mass spring system example. [Wie]. ....	34
Figure 23.	Root locus of the two mass system spring OPLTF. ....	35
Figure 24.	Bode plot of the all-pass nonminimum phase structure filter. ....	36
Figure 25.	Bode plot of the OPLTF of the two-mass-spring system. ....	37
Figure 26.	Impulse response of the CLTF of the two-mass-spring system. ....	38
Figure 27.	Impulse response of the CLTF of the two-mass spring system for 5% increment of the flexibility mode frequency with LQG/LTR. ....	40
Figure 28.	Nyquist plots of the Notch filter system OPLTF for several values of the flexibility mode frequency. ....	42

THIS PAGE INTENTIONALLY LEFT BLANK

## LIST OF TABLES

Table 1.	LQR performance .....	18
Table 2.	Performance of LQG / LTR controller as the process noise increases. ....	26
Table 3.	Variation of Kalman-Bucy filter gain matrices with the process noise increment.....	31
Table 4.	Performance of the LQG/LTR controller for the two-mass spring model.....	39
Table 5.	Notch filter performance for the two-mass spring system.....	41

THIS PAGE INTENTIONALLY LEFT BLANK

## **LIST OF ABBREVIATIONS**

CLTF	Closed Loop Transfer Function
KBF	Kalman-Bucy filter
LQG	Linear Quadratic Gaussian
LQR	Linear Quadratic Regulator
LTR	Loop Transfer Recovery
MIMO	Multiple Input Multiple Output
OPLTF	Open Loop Transfer Function
PI	Proportional Integral
SISO	Single Input Single Output

THIS PAGE INTENTIONALLY LEFT BLANK

## EXECUTIVE SUMMARY

The problem of controlling a rigid body with flexible appendages is presented in this thesis. Of particular application is the control of a satellite with solar panels and various structures and manipulators. The major problem is controlling these flexible appendages to achieve the best performance at minimal cost. The rejection of the overall disturbance is the main purpose of this thesis.

The approach presented is based on the Linear Quadratic Gaussian (LQG) controller with the combination of the Loop Transfer Recovery method. This design is applied to a model by using the state space equations. The model consists of a rigid and a flexible mode characterized by pairs of conjugate poles on the imaginary axis. Using the Matlab Control toolbox, an LQR controller is simulated with feedback states estimated with a Kalman-Bucy filter. Application of the LTR method shows improved robustness in terms of stability margins.

Another approach addressed in this thesis is the application of a structural filter. We show that in one specific example the performance of a nonminimum-phase all-pass filter can be more robust than the LQG/LTR design. The necessary phase shift is obtained by placing zeros in the right half  $s$ -plane. This theory is applied to a single input single output (SISO) system and it is compared with the LQG/LTR technique.

THIS PAGE INTENTIONALLY LEFT BLANK

# I. INTRODUCTION

The problem of controlling systems with flexible structures is of interest in a number of applications. In particular, robotic systems with flexible, lightweight arms and space vehicles with flexible appendages are just a few examples. The challenge of this problem is the fact that the flexible dynamics add modes to the system, which at best degrade the performance and at worst make the system unstable. This is particularly true when the goal of the controller is to drive the system to follow rapid maneuvers, which excite the flexible modes. In this case, the excessive control activity excites vibrations, which can drive the closed loop system to instability.

An example where this class of problem is important is in laser pointing devices deployed in space. This can be the case of laser communication systems or space weapons. The requirements for these applications in general are very stringent, in the sense that the accuracy of the pointing device has to be such as to induce very small tracking errors. This has to be maintained in the presence of a number of perturbations, especially vibrations from various actuators and flexible appendages.

A number of approaches have been presented in the literature. The recent book [Preumont] provides a detailed account of the most important design architectures for a number of applications. The most classical approach is the use of notch filters, tuned at the frequencies of the flexible modes. The goal of this approach is to attenuate the flexible modes in the feedback loop so to prevent self excitation. What is interesting about this approach is that a nonminimum phase design seems to yield best performances, since the extra phase added by the right hand side zero causes a phase shift, which helps to stability of the system. This has been proposed by [Wie] and tested on as simple example. More modern approaches are based on standard state space techniques such as LQR and LQG [Savant]. These controllers perform very satisfactorily and they have a good degree of gain and phase margins.

The problem with the state space approach is that it is sensitive to knowledge of the frequencies of the flexibilities. This constitutes a major obstacle in space applications, since the system cannot be fully tested on the ground and has to be tuned in space. Also, another issue is the fact that the frequencies of the flexible modes vary widely with operating conditions and an exact knowledge is almost impossible.

The goal of this thesis is to address the problem of designing a controller for a flexible system which is robust in the presence of mode uncertainties of the system. The proposed methods are supposed to be developed in conjunction with the frequency estimation of [Tzellos] so that the system can be tuned in an adaptive fashion. The particular methodology is to design an LQG controller with a Loop Transfer Recovery so to improve its gain and phase margins. It is well known that the addition of a Kalman Filter as a state observer greatly affects the stability margins of a LQR state feedback controller. However, even using the estimated state rather than the actual state, satisfactory margins can be obtained by adding an additional noise covariance matrix at the input of the system. This not only improves stability but it seems also to improve the robustness of the system when the flexible modes are uncertain. This technique has been compared with structural notch filters mentioned previously and they both give comparable results. However, what makes the two techniques (notch filters and state space) different is the fact that the notch filter requires tuning which is hard to be automated, while the state space LQG approach comes directly from the solution of a Riccati equation, easy to implement on line.

This thesis is divided into the following chapters. Chapter II develops some of the basic concepts of control theory related to this research. Moreover, we introduce the dynamic model used in this thesis and we develop the equations that describe a flexible structure and the state space models. Chapter III is an overview of LQR design where we examine the application of a LQR controller to the thesis model and its robustness for several values of the nominal frequency of the flexible modes. In Chapter IV, we develop the LQG/LTR design and we examine the performance of this design on the same model. Also, we examine the LQG/LTR controller's behavior as we perturb the flexible mode frequency. In Chapter V, we introduce the concept of the non-minimum phase structural

filter and we examine the stability margins for a specific example. In particular, we compare the robustness of the LQG/LTR controller with that of the structural filter for the same example. A summary of results and recommendations are presented in the last chapter.

THIS PAGE INTENTIONALLY LEFT BLANK

## II. MODELING FOR CONTROL OF FLEXIBLE STRUCTURES

In this chapter, we address some of the basic concepts of control theory applied to flexible structures. In particular, we present the general equations that describe a flexible structure, the state space models and the requirements for stability.

### A. FLEXIBLE STRUCTURE

In this section, we address the problem of modeling a flexible structure. Since the goal is to determine a simple mathematical model that can be used for control design, we need to make a number of assumptions and capture the dominant behavior. Based on these assumptions, a general equation that can describe a flexible structure is

$$L\ddot{x} + A\dot{x} + Bx = Z_u h, \quad (1.1)$$

where the vector  $x$  represents the angular rotation of an element and the vector  $h$  expresses the force or the torque of an actuator. The matrices  $L$ ,  $A$ ,  $B$ ,  $Z_u$  are positive – semi-definite and describe the mass, stiffness, and damping coefficients as well as the force influencing system. These coefficients are approximately known and one approach to define them is by using the Rayleigh damping assumption:

$$A = mL + nB, \quad (1.2)$$

where the  $m$ ,  $n$  coefficients are chosen for the specific model.

The second order differential equation can be transformed into modal coordinates by setting  $x = \Phi \eta$  to become

$$J\ddot{\eta} + 2\Omega\dot{\eta} + \Omega^2\eta = Z_u^T \Phi h, \quad (1.3)$$

where  $\eta$  is a modal vector,  $\Phi$  and  $\Omega$  contain the structural modes and the natural frequencies respectively.

The state space form of equation (1.3) is defined below by setting  $x = \begin{pmatrix} \Omega\eta \\ \dot{\eta} \end{pmatrix}$ , which yields

$$\dot{x} = Mx + Nh, \quad (1.4)$$

where  $M = \begin{pmatrix} 0 & \Omega \\ -\Omega & -2\Omega \end{pmatrix}$  and  $N = \begin{pmatrix} 0 \\ Z_u^T \Phi \end{pmatrix}$ .

The measurements can be defined by the vector  $y$ , which is related to the state as is shown in equation (1.5).

$$y = Gx + Fh, \quad (1.5)$$

where  $G$  is the output matrix and  $F$  a feed-through matrix. [Preumont].

After defining the general mathematical model for a flexible structure, we want to see how the flexible modes affect the s-plane characteristics of the model. In most cases, the flexibility modes appear to have pairs of conjugate poles near the imaginary axis since they correspond to lightly damped vibrations. If not properly taken into account, these modes could make the closed loop system unstable or at least have undesirable behavior. Of course, another set of parameters that we have to take into account is the zeros that are placed on the imaginary axis. In particular, an imaginary zero placed near an imaginary pole can provoke a phase uncertainty for the system's Open Loop Transfer Function (OPLTF) around the frequencies between the zero-pole pair. This situation is known as pole-zero flipping and depends on the relation between the sensor and the actuator. For a collocated structure, where the actuator and the sensor make both the rigid and the flexible mode to co-act stably, the pole-zero flipping situations cannot occur. On the other hand, for a non-collocated structure, where there are some flexible modes that do not co-act with the rigid mode stably, there is a high possibility of pole-zero flipping.

There are some basic design approaches to achieve stability while considering cost minimization. For minimal control effort optimal control theory proposes that poles that are placed on the RHP should be reflected on the stability region to reduce the control energy. It is desirable to least affect any LHP pole, apart from the ones closed to the imaginary axis. Also the designer has to consider that moving the RHP poles into the LHP affects the system's bandwidth and its sensitivity to noise. [Savant-Preumont-Wie].

A typical pole-zero configuration of a flexible system is indicated in Figure 1.

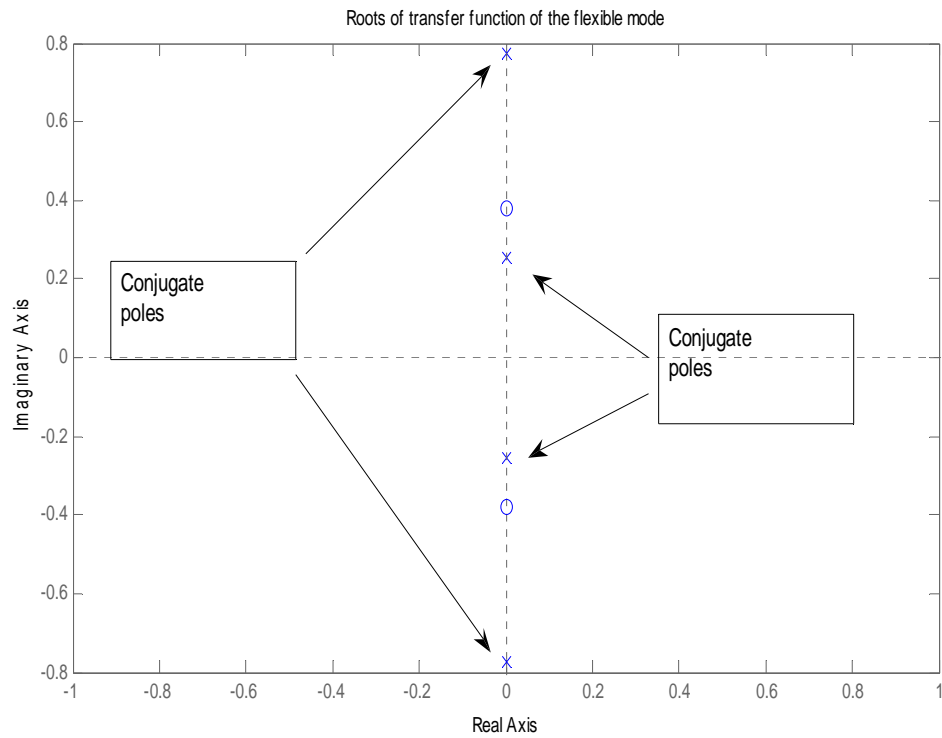


Figure 1. Pole-zero map of a flexible mode.

## B. STATE SPACE MODELING

A state space model decomposes  $n$ th-order differential equations into  $n$  first-order differential equations. In particular, let  $x(t)$  be the state at time  $t$ ; then a system can be represented as indicated in Figure 2.

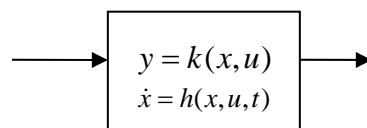


Figure 2. State Space Model. [Hespanha].

The vectors  $x, u, y$  correspond to the state, input and output vectors respectively. The function  $h$  relates the first derivative of the state vector with the state vector itself and the input vector, and the function  $k$  relates the output vector with the input and state vector. In the case of a linear time invariant Single Input Single Output (SISO) system, the state space model has the following form:

$$\dot{x} = Ax + Bu \quad (1.6)$$

$$y = Cx + Du, \quad (1.7)$$

where  $x$  is the state vector,  $u$  is the input vector and  $y$  is the output vector.  $A$  is the system matrix,  $B$  the input matrix,  $C$  the output matrix and  $D$  is a feed-through matrix. The  $D$  matrix is usually set to zero since there is always a reaction time between input and output.

The system's transfer function can be determined by applying the Laplace transform on equations (1.6), (1.7). Assuming there are no feed-through terms, i.e.,  $D = 0$ , we obtain:

$$sX(s) - x(0) = AX(s) + BU(s) \quad (1.8)$$

$$Y(s) = CX(s). \quad (1.9)$$

Setting the initial conditions to zero  $x(0) = 0$

$$X(s) = (sI - A)^{-1}BU(s) \quad (1.10)$$

and combining with the output equation we obtain

$$Y(s) = C(sI - A)^{-1}BU(s). \quad (1.11)$$

This yields the transfer function

$$H(s) = C(sI - A)^{-1}B. \quad (1.12)$$

The model that is used in this thesis is a SISO system representing the behavior of a flexible space structure. In particular, it consists of a rigid and a flexible body connected in series as indicated in Figure 3.

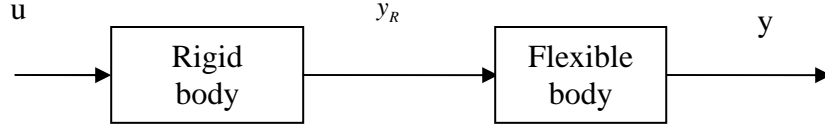


Figure 3. Model representation.

If we separate the state into the rigid and the flexibility components, we obtain the two state-space models:

$$\dot{x}_R = A_R x_R + B_R u_R \quad (1.13)$$

$$y_R = C_R x_R \quad (1.14)$$

and

$$\dot{x}_F = A_F x_F + B_F u_F \quad (1.15)$$

$$y_F = C_F x_F. \quad (1.16)$$

In a cascade model the input of the flexible mode is the output of the rigid mode, so  $y_R = u_F$ .

Let  $\dot{x} = \begin{pmatrix} \dot{x}_R \\ \dot{x}_F \end{pmatrix}$  then the overall state space model is obtained as

$$\dot{x} = \begin{pmatrix} A_R & O \\ B_F C_R & A_F \end{pmatrix} \begin{pmatrix} x_R \\ x_F \end{pmatrix} + \begin{pmatrix} B_R \\ O \end{pmatrix} u \quad (1.17)$$

$$y = \begin{pmatrix} O & C_F \end{pmatrix} \begin{pmatrix} x_R \\ x_F \end{pmatrix}, \quad (1.18)$$

where  $O$  is a zero matrix,  $A_R$  and  $A_F$  are the state matrices,  $B_R$  and  $B_F$  are the input matrices,  $C_R$  and  $C_F$  are the output matrices of the rigid and flexible modes respectively.

The transfer function of the system is

$$H(s) = C_s (sI - A_s)^{-1} B_s, \quad (1.19)$$

where  $A_s = \begin{pmatrix} A_R & O \\ B_F C_R & A_F \end{pmatrix}$ ,  $B_s = \begin{pmatrix} B_R \\ O \end{pmatrix}$ ,  $C_s = \begin{pmatrix} O & C_F \end{pmatrix}$  and  $I$  is the identity matrix.

The example used in this thesis is described by the equations (1.13)-(1.18) by setting  $A_R = \begin{pmatrix} 0 & 0 \\ 1 & 0 \end{pmatrix}$ ,  $B_R = (10)$  and  $C_R = (01)$  for the rigid body mode and

$$A_F = \begin{pmatrix} 0 & -0.6638 & 0 & -0.3120 \\ 1.00 & 0 & 0 & 0 \\ 0 & 0.50 & 0 & 0 \\ 0 & 0 & 0.25 & 0 \end{pmatrix}, B_F = \begin{pmatrix} 0.0625 \\ 0 \\ 0 \\ 0 \end{pmatrix} \text{ and } C_F = (0 \ -0.0560 \ 0 \ -0.0640)$$

for the flexible mode.

### III. STATE FEEDBACK / LINEAR QUADRATIC REGULATOR

In this chapter, we recall control design techniques based on state feedback theory and the Linear Quadratic Regulator (LQR). We begin by identifying the phase (PM) and gain (GM) margins of the LQR approach and follow up by experimenting with the system's robustness.

#### A. STABILITY

A fundamental objective in control system design is the stability of the system. By the Nyquist criterion we can assess closed loop stability. In particular the number of RHP poles of the Closed Loop Transfer (CLTF) is equal to the sum of the number of the clockwise encirclements of the -1 point on the s-plane and the number of RHP poles of the OPLTF.

#### B. OPTIMIZATION / LINEAR QUADRATIC (LQR) REGULATOR

By the process of optimization, we design a control system by minimizing a cost function,  $J$ , which can be described by the equation (2.1).

$$J = \int L(x, u, t) dt, \quad (1.20)$$

where the state vector  $x$  is related to the input vector  $u$  by a first order differential equation

$$\dot{x} = f(x, u, t). \quad (1.21)$$

A well-known result is that we minimize the cost function  $J$  by the LQR. Let the state space model be:

$$\dot{x} = A_s x + B_s u \quad (1.22)$$

$$y = C_s x \quad (1.23)$$

and the cost function to be minimized

$$J = \int (x^T Q x + u^T R u) dt, \quad (1.24)$$

where  $Q$  is a positive semi-definite matrix known as the state weighting matrix and  $R$  is

a positive definite matrix known as control weighting matrix. These matrices are selected by the designer and have a deterministic role in finding the optimal gain for the LQR problem.

The solution to this problem is a gain matrix,  $L$ , that is calculated from the equation

$$L = R^{-1}B^TW, \quad (1.25)$$

where  $W$  satisfies the Algebraic Riccati Equation

$$WA + A^TW - WBR^{-1}B^TW + Q = 0. \quad (1.26)$$

Finally the input  $u$  of the control system has the form of:

$$u = -Lx + r \quad (1.27)$$

with  $r$  being an external command signal.

Figure 4 shows the block diagram of the state feedback LQR for the model in this thesis.

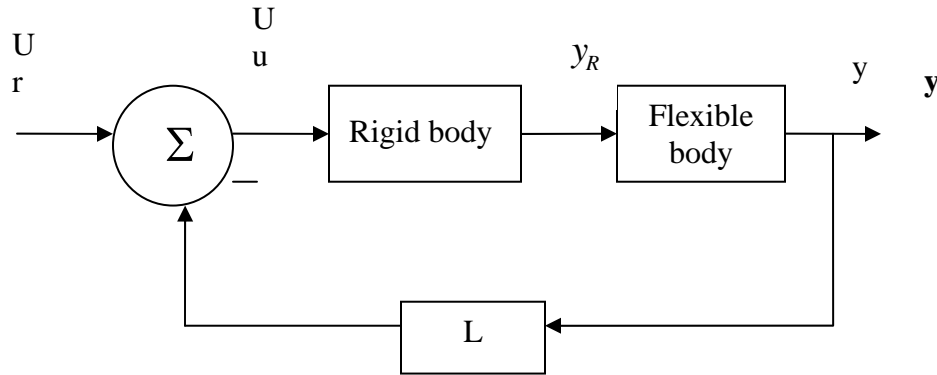


Figure 4. Linear Quadratic Regulator Block Diagram.

The OPTLT of this system can be determined as in the state space model presentation and is:

$$H(s) = L(sI - A_s)^{-1}B_s. \quad (1.28)$$

The LQR approach is commonly used for designing state feedback controllers because of its ability to guarantee robust stability even in the presence of model uncertainties. This is because the LQR has a PM  $>60^\circ$  and an infinite GM, thus

guaranteeing robustness of the system in the presence of perturbations. However, a major drawback of this design is that the LQR needs the feedback state vector to be available, which, in many real time applications, is not feasible. [Preumont].

The LQR properties can be verified from the model of this thesis. More specifically, if we use the example of page (6) then the model shows a PM of  $62^\circ$  and an infinite GM as indicated in Figure 5.

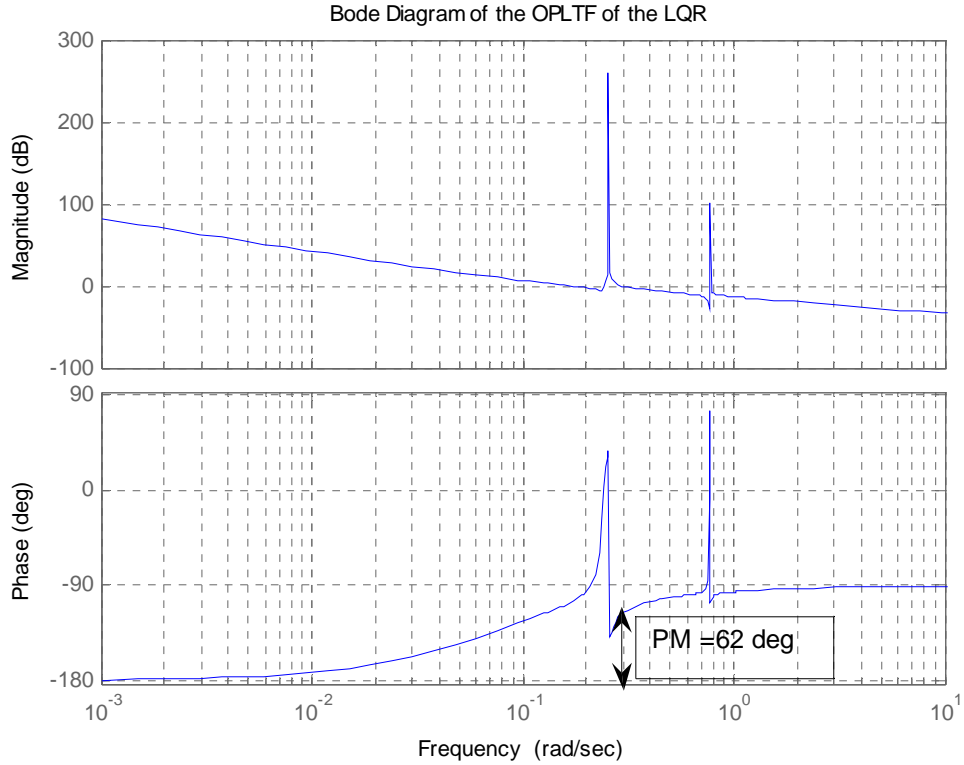


Figure 5. Bode plot of OPLTF of the LQR design in the nominal frequency

As mentioned earlier, the computation of the gain matrix  $L$  requires the solution of the Algebraic Riccati Equation, which depends on the  $R$  and  $Q$  matrices. For this thesis these two matrices have been selected to be

$$R=1 \text{ and } Q=C_s C_s^T.$$

The system is stable and Figure 6 shows the impulse response of the CLTF, which, as expected, decays to zero.

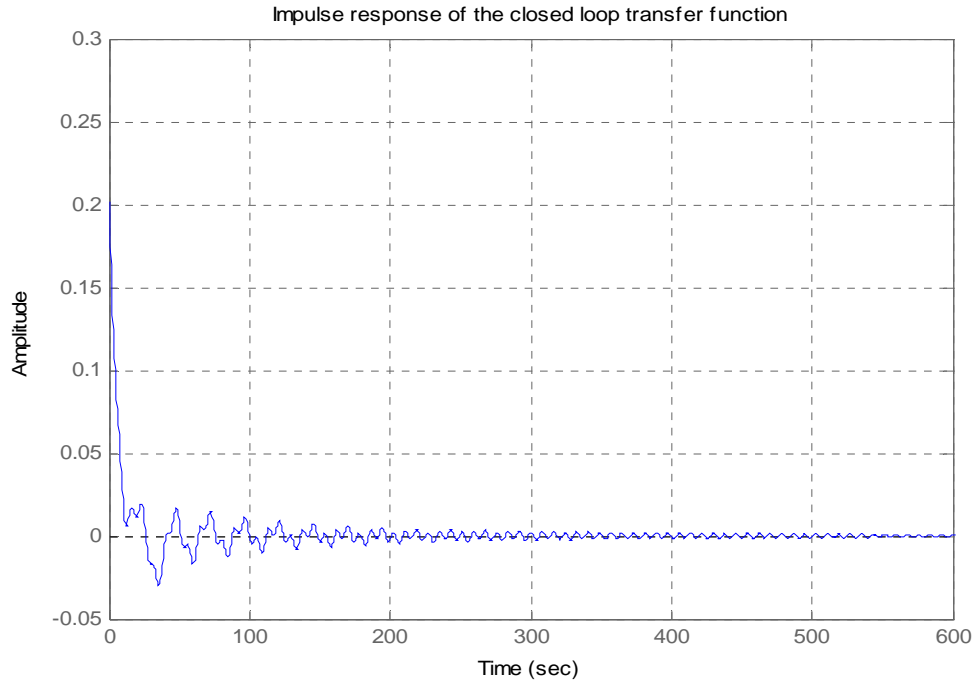


Figure 6. Impulse Response of the LQR CLTF.

### C. ROBUSTNESS / STABILITY OF LQR DESIGN

In this section, we examine the ability of the LQR approach to retain the model's stability in the presence of perturbations. In particular, we show how the increase of the frequency in the flexible mode affects the PM and the GM of the system and how the system responds to these changes. In order to compare the different cases we used a number of plots in which the frequency flexibility mode varies between within 5%, 10% and 20%, respectively, as shown in Figures 7, 8, and 9.

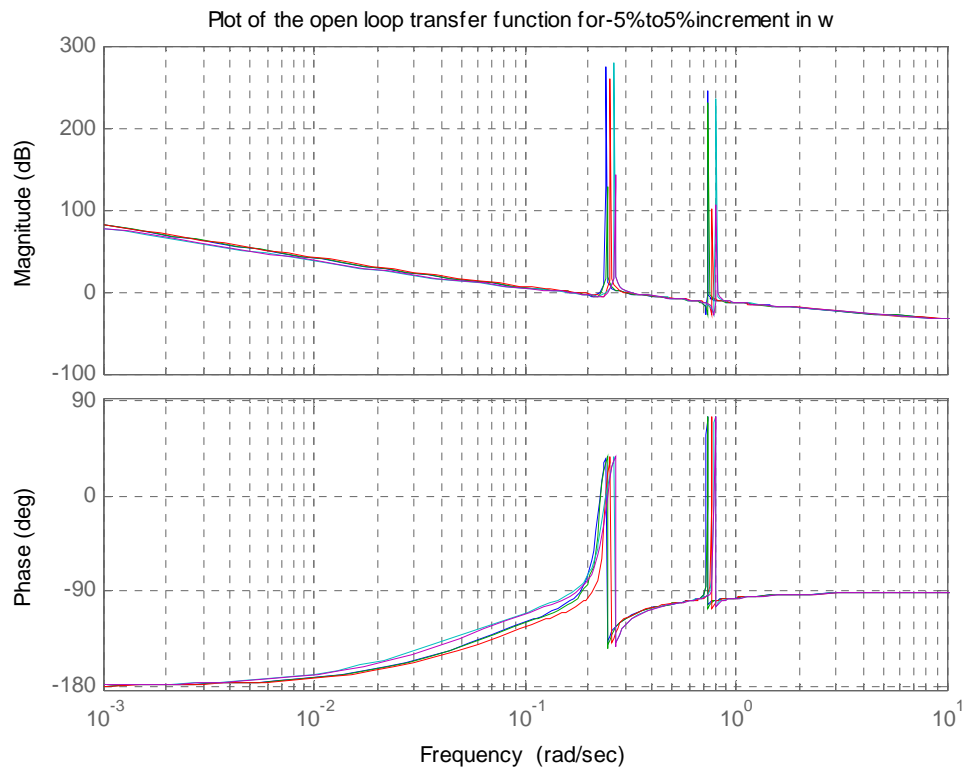


Figure 7. Bode plot of OPLTF in the presence of -5% to 5% increment of the nominal frequency.

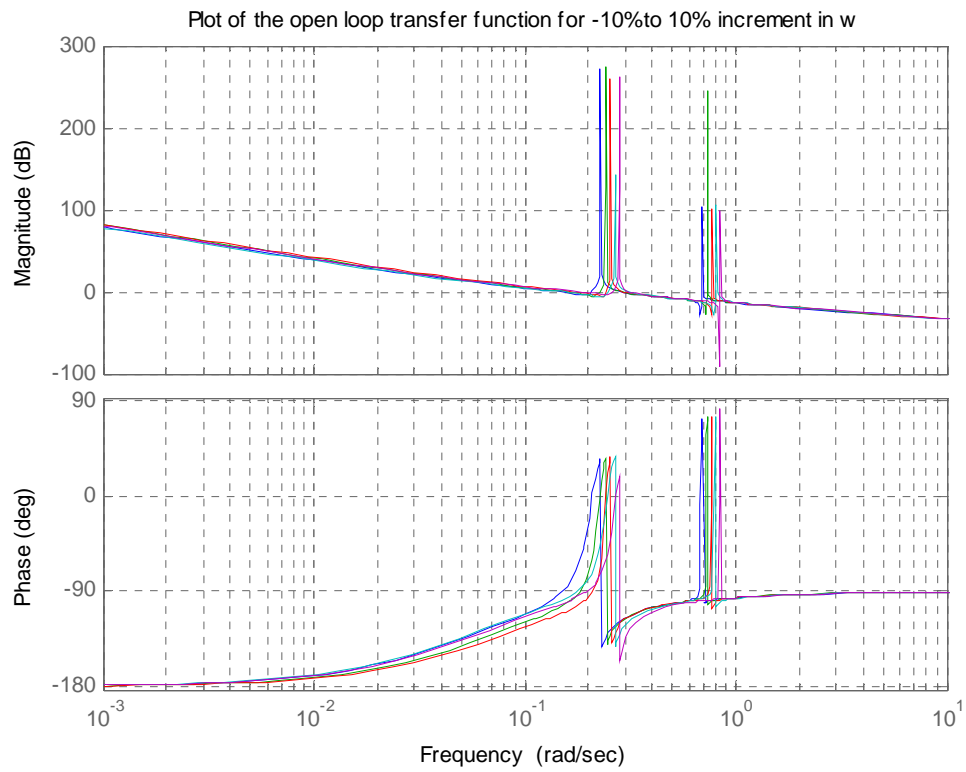


Figure 8. Bode plot of OPLTF in the presence of -10% to 10% increment of the nominal frequency.

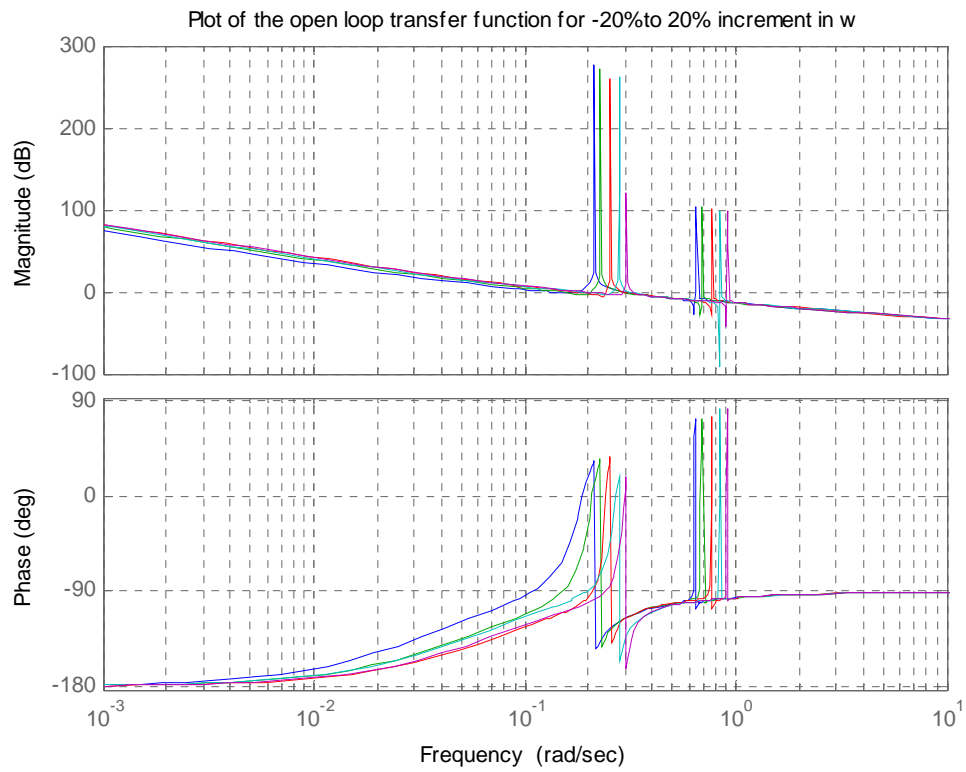


Figure 9. Bode plot of OPLTF in the presence of -20% to 20% increment of the nominal frequency.

Table 1 shows the stability margin variations in connection with the percent perturbation of the flexibility's nominal frequency.

<b>LQR Controller</b>				
<b>% increment in the nominal frequency</b>	<b>5</b>	<b>10</b>	<b>15</b>	<b>30</b>
<b>PM (degrees)</b>	<b>61.2</b>	<b>51.3</b>	<b>50.4</b>	<b>48</b>
<b>GM (dB)</b>	$\infty$	$\infty$	$\infty$	$\infty$
<b>Gain Cross Over frequency (Hz)</b>	<b>0.3104</b>	<b>0.312</b>	<b>0.3187</b>	<b>0.3375</b>
<b>Phase Cross Over frequency (Hz)</b>	$\infty$	$\infty$	$\infty$	$\infty$

Table 1. LQR performance

In all cases, we notice that there is sufficient margin (phase and gain) to ensure closed loop stability in the presence of model uncertainties.

## IV. LINEAR QUADRATIC GAUSSIAN / LOOP TRANSFER RECOVERY DESIGN (LQG/LTR)

This chapter analyzes the Linear Quadratic Gaussian and Loop Transfer Recovery design (LQG/ LTR) and its performance. Moreover, we present the LQG control design and we examine its stability in the presence of flexible modes. Also, we introduce the Loop Transfer Recovery (LTR) method and its performance at the stability margins of the LQG controller.

### A. LINEAR QUADRATIC GAUSSIAN (LQG)

In most applications, the state vector is not available since this would require an excessive number of sensors. Thus, the feedback states have to be estimated. This leads to the LQG controller, which consists of an LQR controller and a Kalman-Bucy filter for the state feedback estimation.

Consider the linear time invariant system:

$$\dot{x} = Ax + Bu + w \quad (2.1)$$

$$y = Cx + v, \quad (2.2)$$

where  $w$  and  $v$  are the process and the measurement noise respectively. It is convenient to assume that these noises are Gaussian, white with zero mean. The optimal gain matrix of the filter can be computed by the following equation:

$$K = NC^T R^{-1}, \quad (2.3)$$

where the matrix  $N$  is the solution of the algebraic Riccati equation:

$$AN + NA^T - NCR_0^{-1}C^T N + Q_0 = 0. \quad (2.4)$$

The matrices  $R_0$   $Q_0$  are known as the covariance matrices and they refer to the noise parameters of the system. They are usually provided by the designer and they model the noise intensity level. Since they are covariance matrices,  $R_0$   $Q_0$  have to be positive definite and positive semi-definite, respectively, for the Riccati Equation to be solvable. [Savant].

In order to analyze the robustness of the LQG design we need to look at the open loop dynamics and its stability margins. Of particular interest, is the open loop frequency response we obtain by breaking the loop at the point **X** as illustrated in Figure 10.

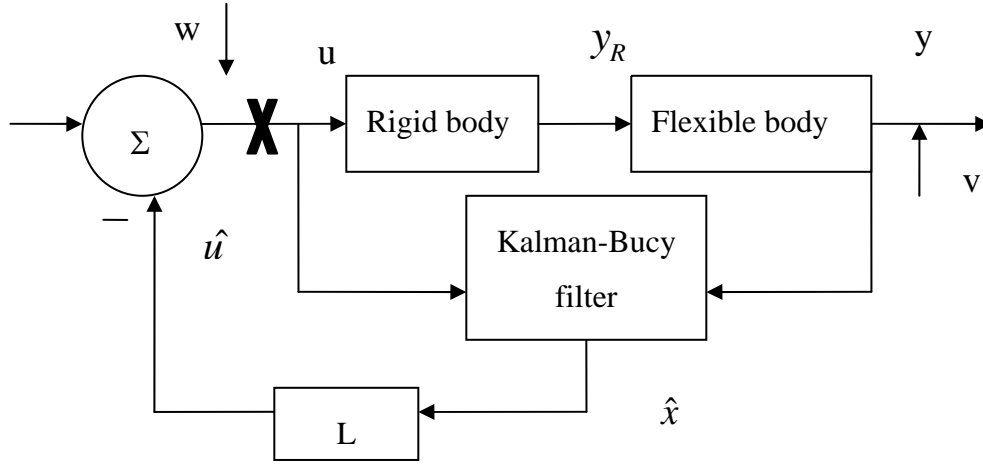


Figure 10. Linear Quadratic Gaussian Block Diagram.

From the state space model of the system we obtain

$$\dot{x} = A_s x + B_s u + w \quad (2.5)$$

$$y = C_s x + v. \quad (2.6)$$

The Kalman-Bucy filter and the control input combined yield

$$\dot{\hat{x}} = A_s \hat{x} + B_s u + K(y - C_s \hat{x}) - BL\hat{x} \quad (2.7)$$

$$\hat{u} = -L\hat{x}. \quad (2.8)$$

If we set  $\dot{x}_s = \begin{pmatrix} \dot{x} \\ \dot{\hat{x}} \end{pmatrix}$  then the overall system's state space equations can be written as indicated below:

$$\dot{x}_s = \begin{pmatrix} A_s & O \\ KC_s & A_s - KC_s - B_s L \end{pmatrix} \begin{pmatrix} x \\ \hat{x} \end{pmatrix} + \begin{pmatrix} B_s \\ O \end{pmatrix} u \quad (2.9)$$

$$\hat{u} = (OL) \begin{pmatrix} x \\ \hat{x} \end{pmatrix}. \quad (2.10)$$

Finally, the OPLTF between  $u$  and  $\hat{u}$  in Figure 10 can be computed from equation (3.11)

$$H(s) = L(sI - A_s + B_s L + K C_s)^{-1} K C_s (sI - A_s)^{-1} B_s. \quad (2.11)$$

Once more, if we apply the LQG design in the example that we described in Section I, p. 6, we can see that the system is stable and the impulse response of the CLTF decays to zero, as illustrated in Figure 11.

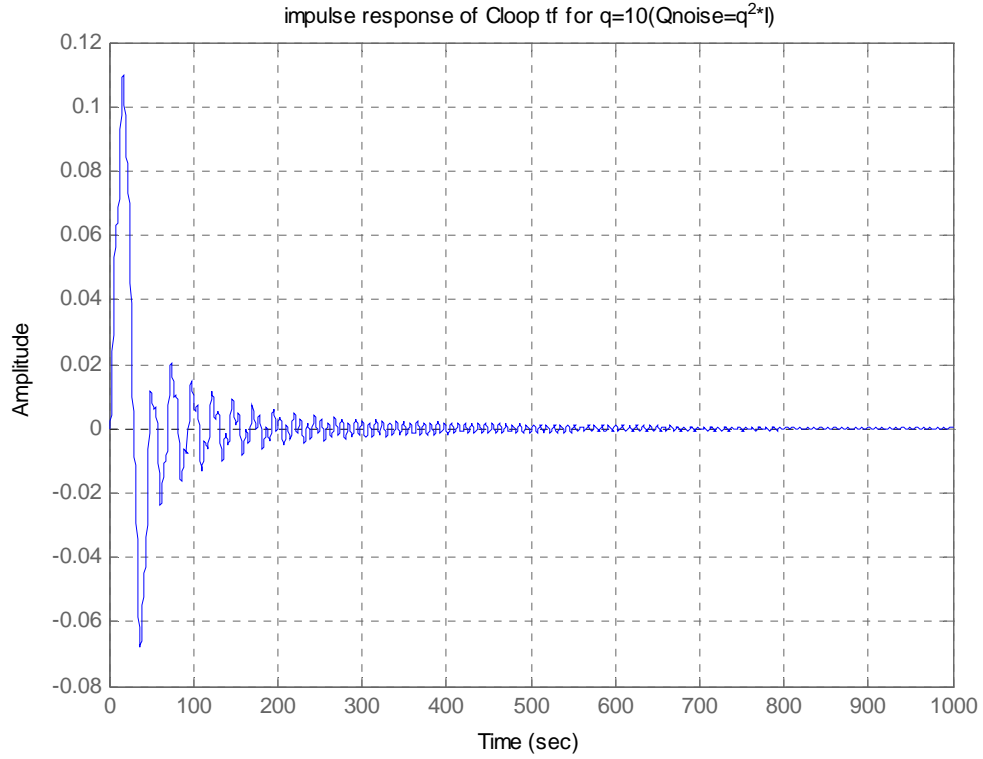


Figure 11. Impulse response of the LQG CLTF.

However, the PM and the GM of the system have decreased considerably. In fact, the PM became  $30^0$  and the GM equal to 1.88 db as we can see from Figure 12. This means that the sensitivity of the LQG design in the noise parameters has increased and there is a possibility of losing the stability of the system.

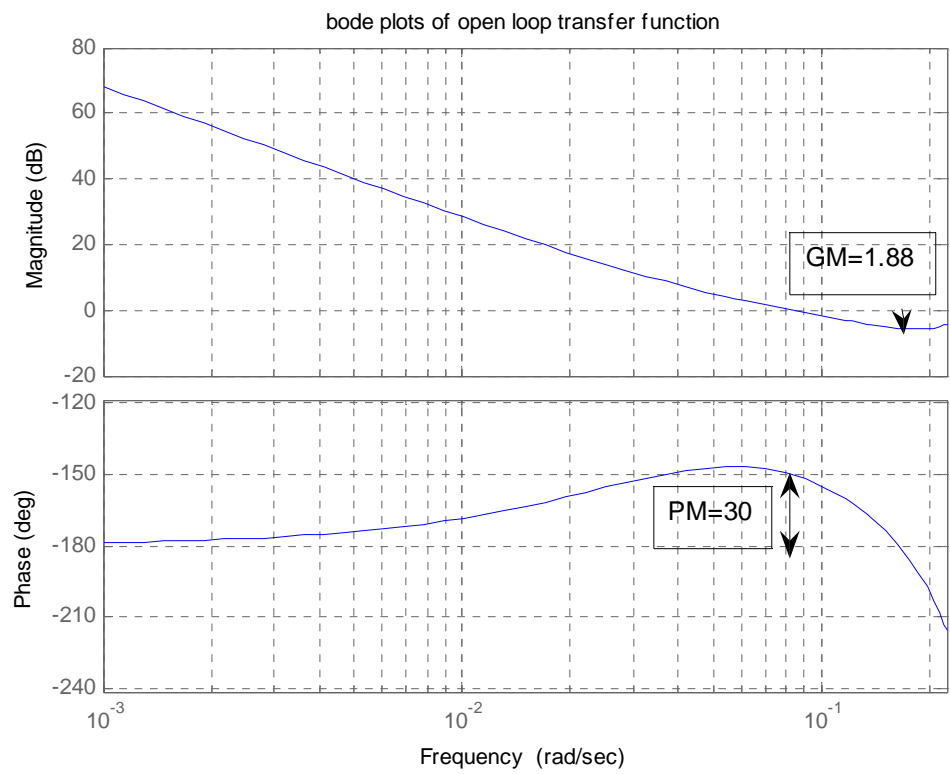


Figure 12. Bode plot of OPLTF of the LQG design.

Indeed, if the gain matrices  $L$  and  $K$  remain constant and the flexibility mode frequency is increased by 5%, then the system can become unstable. This is shown in Figure 13 and Figure 14, where the CLTF and the Bode plot OPLTF of the system are indicated.

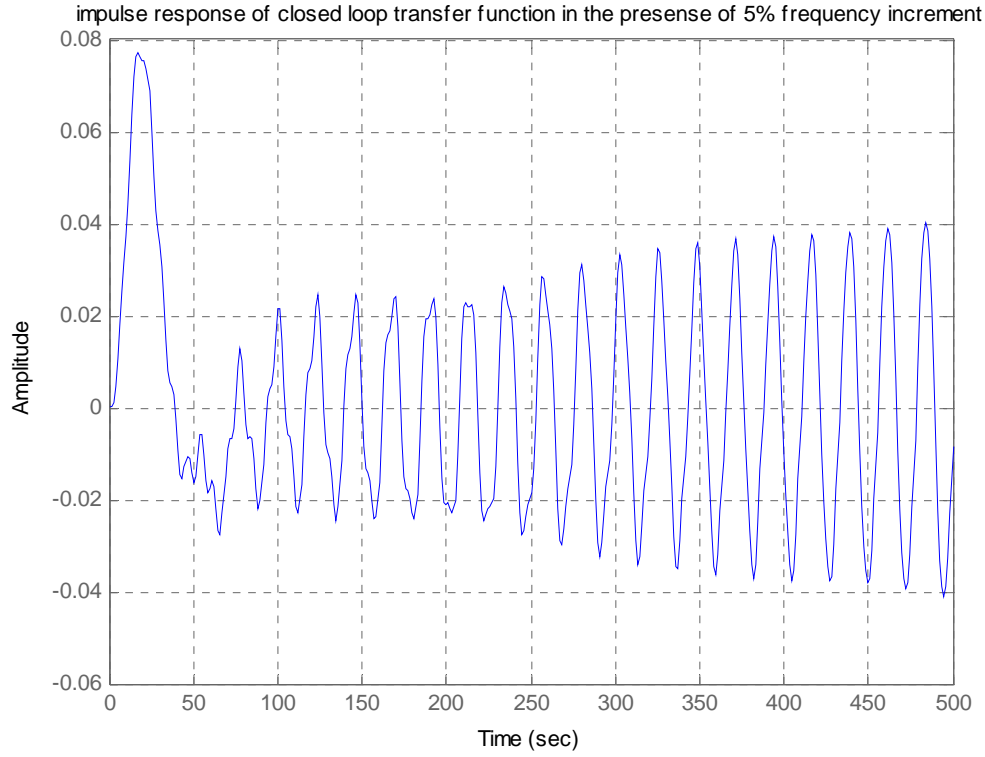


Figure 13. Impulse response of the CLTF of the LQG design in the presence of 5% increment in the frequency of the flexible mode.

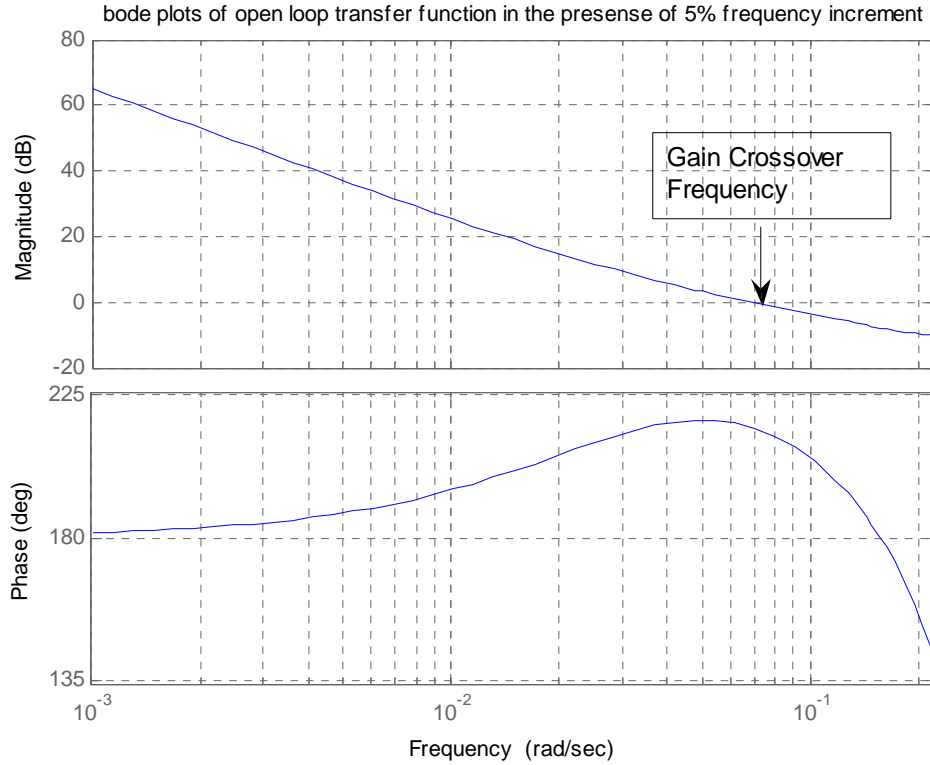


Figure 14. Bode plot of the OPLTF of the LQG design in the presence of 5% increment of the flexible mode frequency.

## B. LOOP TRANSFER RECOVERY

As mentioned in Chapter II, the LQR procedure guarantees a PM of 60 degrees and an infinite GM. In spite of the excellent stability, the LQR is not a viable solution to the control problem because it requires that all states are available. The use of a Kalman filter to predict the system's states was a good solution to this problem but had as an impact the loss of LQR properties. Doyle and Stein [Savant] developed a method that, under specific conditions, ensures that the LQG shows approximately the same behavior as the LQR.

The Loop Transfer Recovery (LTR) is based on the configuration of the LQG design. More specifically, the noise covariance matrices  $R_0$   $Q_0$  can play a deterministic role in the LTR procedure. Recall that the OPLTF of the LQR and LQG respectively are given by:

$$H(s)_{LQR} = L(sI - A_s)^{-1} B_s \quad (2.12)$$

$$H(s)_{LQG} = L(sI - A_s + B_s L + K C_s)^{-1} K C_s (sI - A_s)^{-1} B_s. \quad (2.13)$$

It can be proved that when the system has no zeros in the RHP and the noise covariance matrices are chosen to be  $R_0 = 1$  and  $Q_0 = g^2 B B'$  the LQG converges to the LQR as

$$\lim_{g \rightarrow \infty} H(s)_{LQG} = H(s)_{LQR}, \quad (2.14)$$

where  $g$  is a scalar arbitrary variable. As a consequence, the LTR method guarantees that as the process noise is increased, the LQG recovers the LQR robustness properties. Of course, for  $g = 0$  the KBF has the nominal value for the true noise intensities. As  $g$  increases, the filter efficiency is getting smaller but the PM and the GM is improved providing a response less sensitive to modeling errors. [Savant].

This statement can be verified from Table 2, where the reader can see that margin stabilities are increasing and that the LQG/LTR method satisfies the convergence criterion. The matrix values came from the application of the LQG/LTR design in the example of Chapter I, p. 6.

<b>LQG / LTR Controller</b>				
<b>increment in the scalar g</b>	<b>10</b>	<b>100</b>	<b>1000</b>	<b>10,000</b>
<b>PM (degrees)</b>	<b>34.58</b>	<b>40.5371</b>	<b>45.8733</b>	<b>51.2310</b>
<b>GM (dB)</b>	<b>1.98</b>	<b>2.6967</b>	<b>4.2328</b>	<b>6.4818</b>
<b>Gain Cross Over frequency (Hz)</b>	<b>0.2130</b>	<b>0.3609</b>	<b>0.7336</b>	<b>0.7572</b>
<b>Phase Cross Over frequency (Hz)</b>	<b>0.1102</b>	<b>0.2722</b>	<b>0.2789</b>	<b>0.2834</b>

Table 2. Performance of LQG / LTR controller as the process noise increases.

This convergence can be seen by comparing the Bode plots of the OPLTF of the LQR and the OPLTF of the LQG/LTR controllers on the same example.

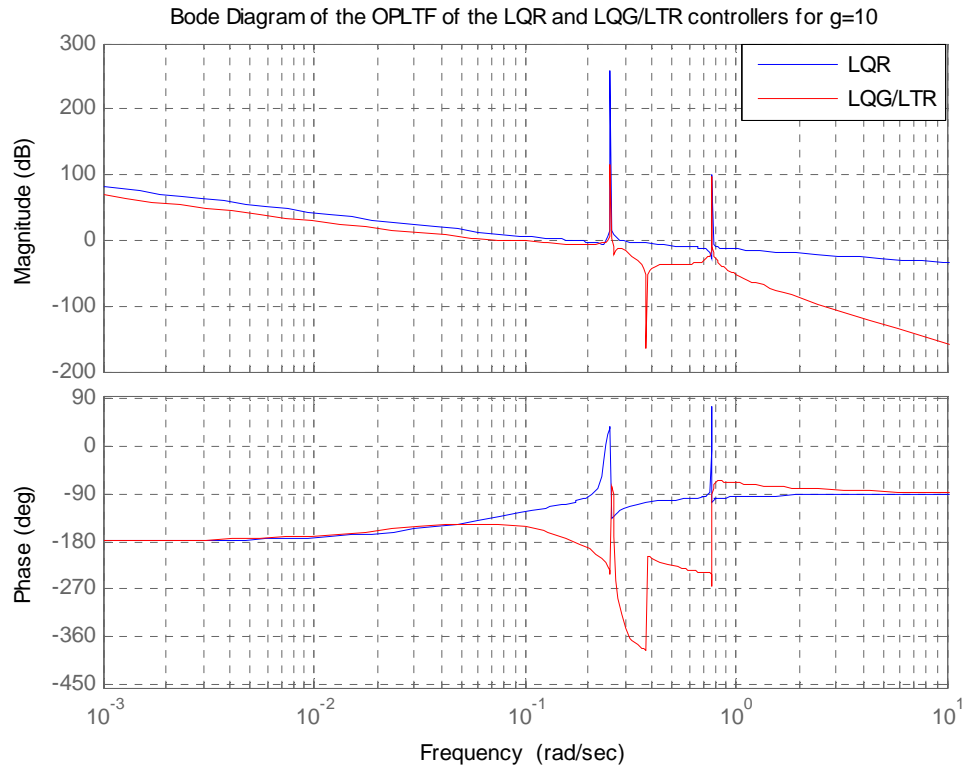


Figure 15. Bode plots of OPLTF of the LQR and the LQG/LTR controllers for  $g=10$ .

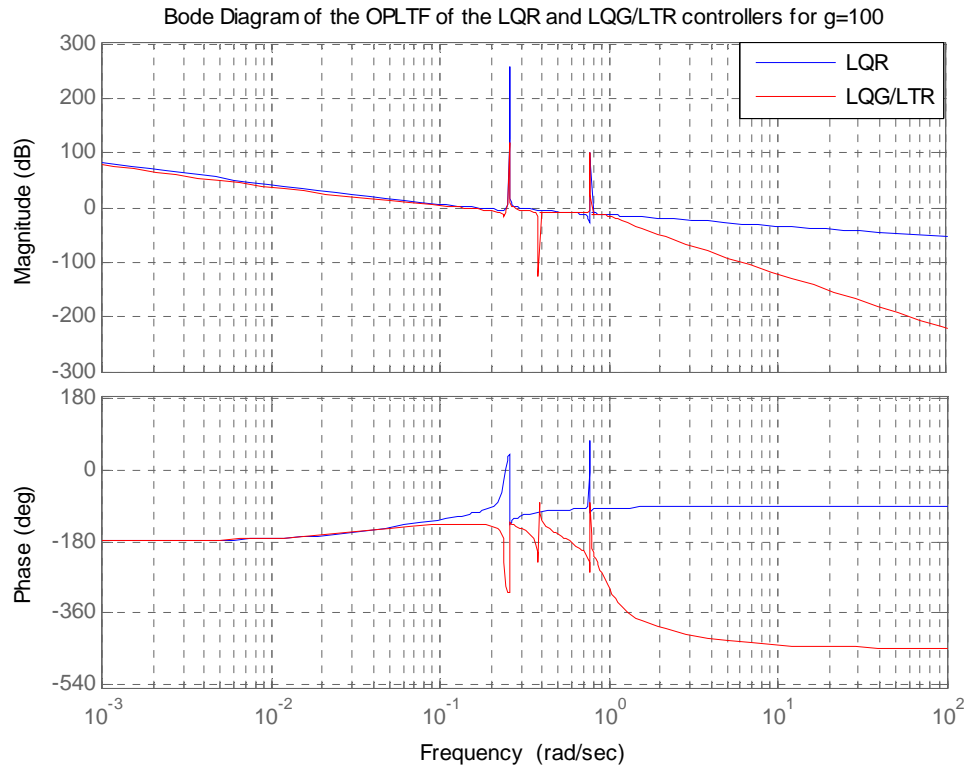


Figure 16. Bode plots of OPLTF of the LQR and the LQG/LTR controllers for  $g=100$ .

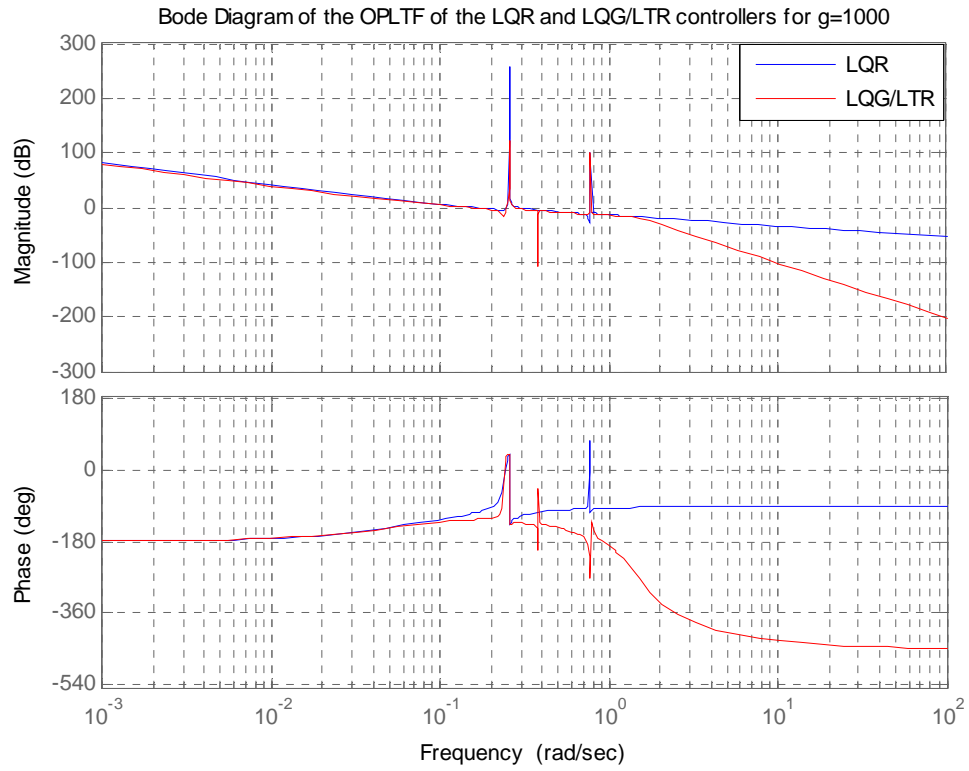


Figure 17. Bode plots of OPLTF of the LQR and the LQG/LTR controllers for  $g=1000$ .

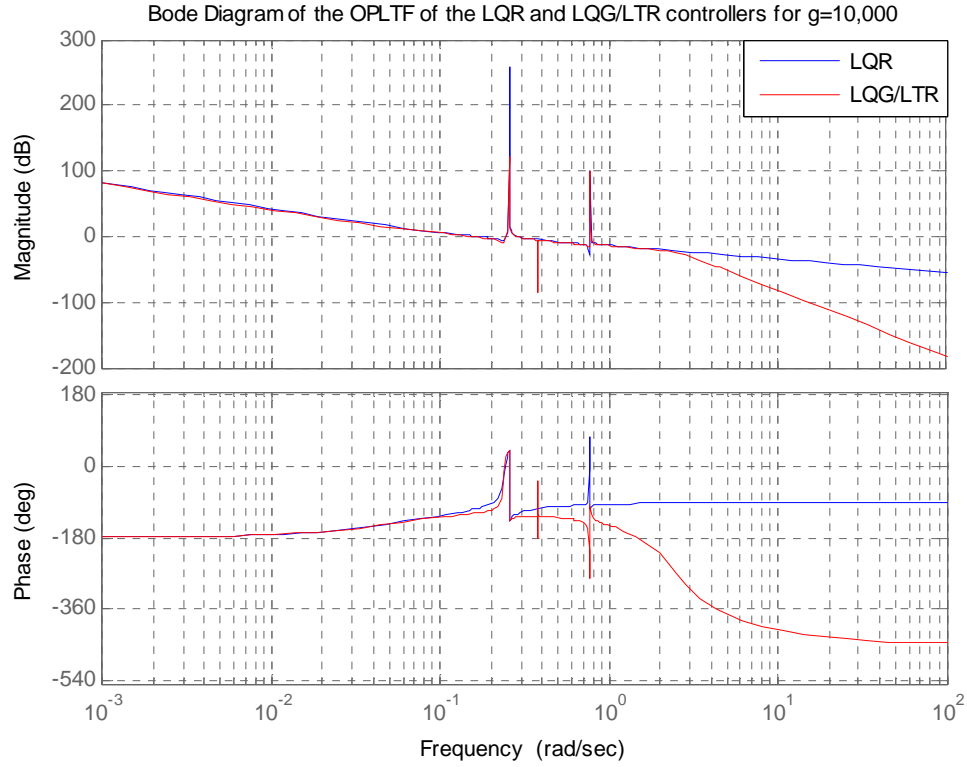


Figure 18. Bode plots of OPLTF of the LQR and the LQG/LTR controllers for  $g=10,000$ .

From Figures 15-18, we can see that as the process noise is increased, the LQG/LTR converges to the LQR plot in magnitude and phase.

Another issue that has to be examined is the robustness of this method. Having calculated the Kalman filter gain matrices  $K$  for every variation of the scalar  $g$ , as indicated in Table 3, the model is tested for its stability every time the perturbation frequency is increased.

Kalman-Bucy filter gain matrices					
increment in the scalar $g$	1	10	100	1000	10,000
Gain matrix $K$	-1.0000 -13.833 0.0624 0.1300 -1.4937 -3.2701	-10.000 -67.607 -0.3357 -4.9828 -11.608 -5.6335	-100.0000 -339.3195 -17.2514 -29.3866 -17.7253 1.0111	1.0e+003* [-1.0000 -1.8830 -0.0943 -0.0644 -0.0149 0.0044]	1.0e+004* [-1.0000 -1.0672 -0.0341 -0.0117 -0.0012 0.0005]

Table 3. Variation of Kalman-Bucy filter gain matrices with the process noise increment.

Also, Table 3 shows that the drawback of the LTR is an increase in the gain matrix  $K$ , thus increasing the sensitivity to measurement noise.

In Figure 19, we show the Nyquist plots of the LQG/LTR controller OPLTF for several values of the parameter  $g$  at the nominal frequency. It can be seen that none of the plots crosses the -1 point, thus guaranteeing closed loop stability.

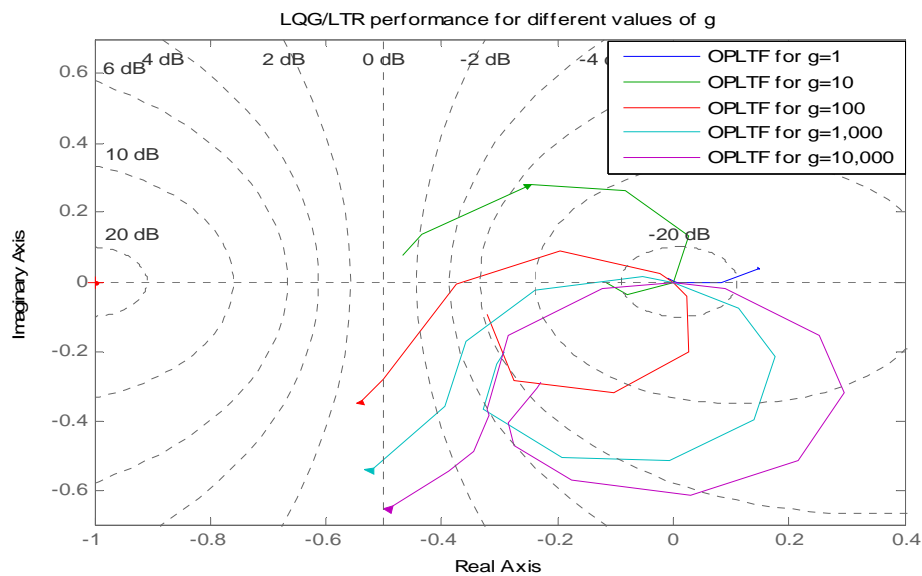


Figure 19. Nyquist plot of the OPLTF at the nominal frequency for several values of  $g$ .

As the nominal frequency is increased, the plots tend to get closer to the -1 point. In Figure 20, we show the Nyquist plots of the OPLTF for 10% increment of the nominal frequency. The plot that corresponds to the OPLTF with  $g = 1$  crosses the -1 point and provides instability into the system.

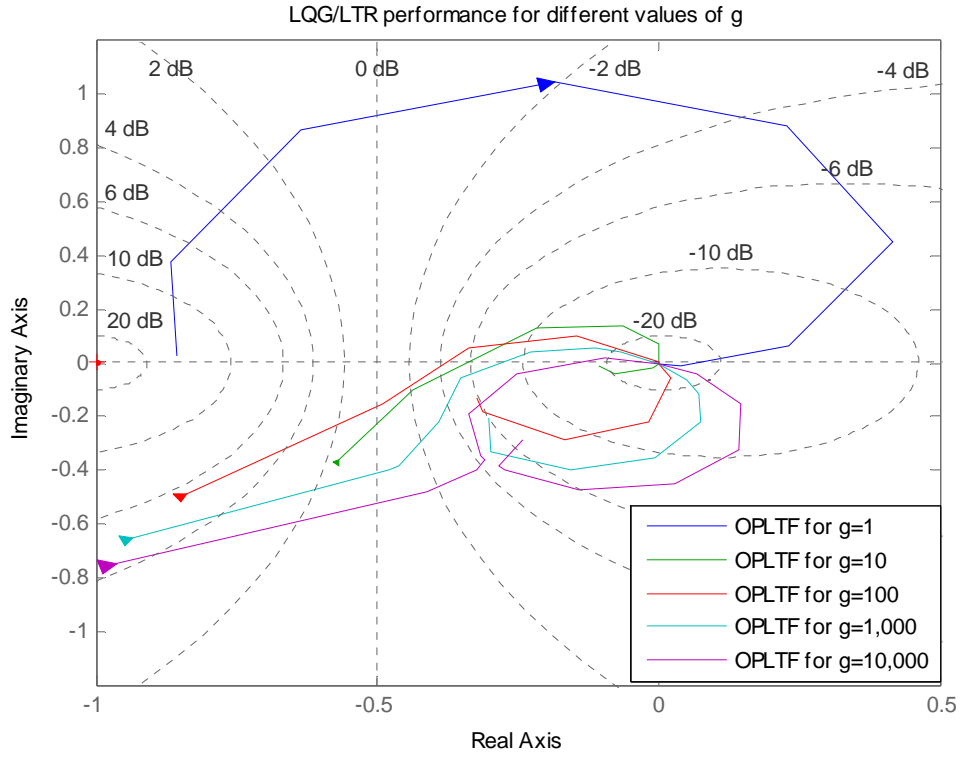


Figure 20. Nyquist plot of the OPLTF at the presence of 10% increment of the nominal frequency for several values of  $g$ .

## V. STRUCTURAL FILTER DESIGN

In this chapter, we analyze the concept of a structural second order nonminimum-phase filter and its performance on a model that has a pair of conjugate poles on the imaginary axis of the s-plane as shown in Figure 21. Also, the model is tested with the LQG/LTR method and a comparison between the results of these two is presented.

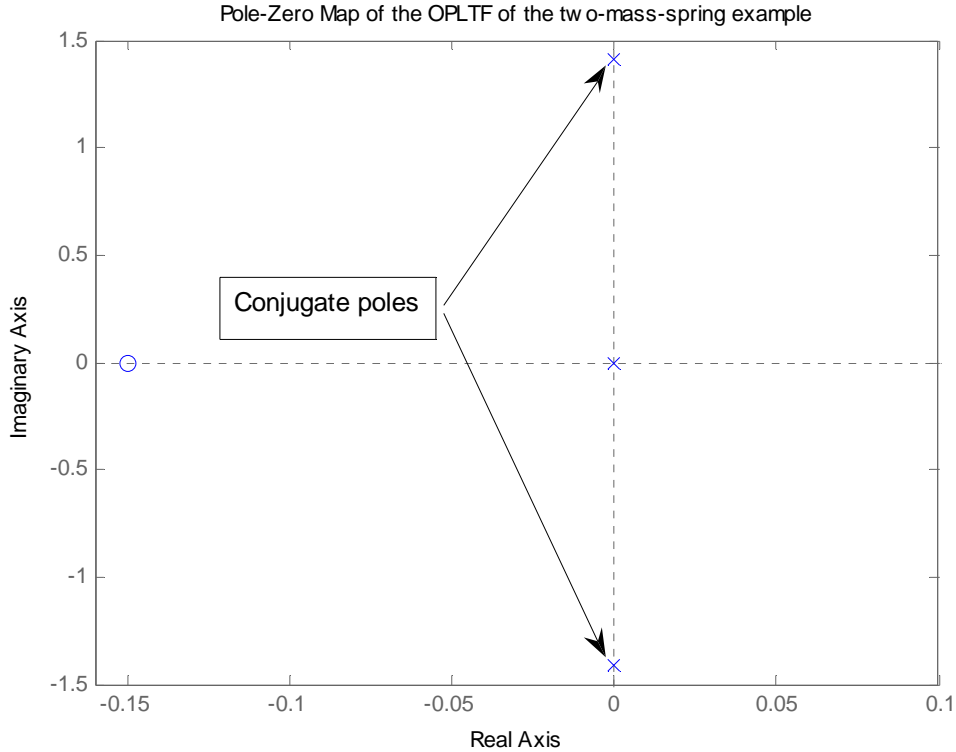


Figure 21. Pole-Zero map of the OPLTF of the two-mass-spring example.

### A. NON MINIMUM PHASE STRUCTURE FILTER

The concept of the nonminimum-phase structural filter is a particular case of the common notch filter that is characterized by a specific property. First of all, it is a second order filter with transfer function described as follows:

$$H(s) = \frac{s^2 / \omega_z^2 + 2\zeta_z s / \omega_z + 1}{s^2 / \omega_p^2 + 2\zeta_p s / \omega_p + 1}. \quad (2.15)$$

The terms  $\omega_z, \zeta_z, \zeta_p$  and  $\omega_p$  define the filter's coefficients and, for any variation of the above terms, there are shaped filters with specific frequency responses. So, it can be formatted as a band-pass, a low-pass, or a high-pass filter. Another basic property is that the zeros of the transfer function can be placed on the RHP. The purpose of this technique is to decrease the counteraction of the flexible modes by providing the suitable phase alteration into the system. [Wie].

To understand better the performance of the structural filter, an example of two bodies that are connected by a spring with constant  $k$  is described bellow.

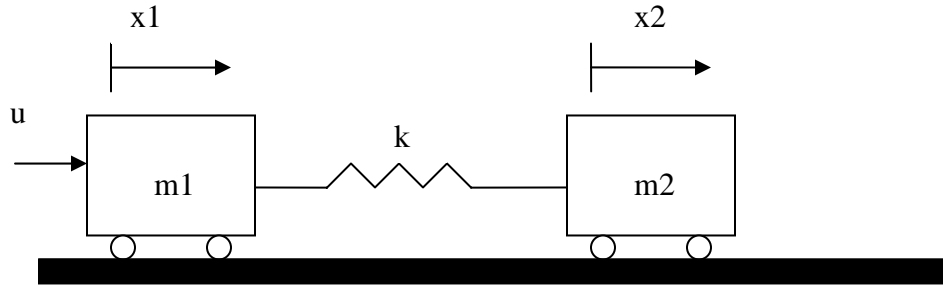


Figure 22. Two mass spring system example. [Wie].

The masses of the two bodies and the constant  $k$  are selected to be equal to 1. On the first body, a force acts and this action is transferred to the second body through the spring. In this example, we measure only the position  $x_2$  and its first derivative. The transfer function of this system is:

$$\begin{bmatrix} x_1(s) \\ x_2(s) \end{bmatrix} = \frac{1}{s^2(s^2 + 2K)} \begin{bmatrix} s^2 + K \\ K \end{bmatrix} u(s). \quad (2.16)$$

Also, for the rigid body, a proportional integral (PI) compensator is designed with the following transfer function:

$$C(s) = 0.086(s/0.15 + 1). \quad (2.17)$$

The interaction between the flexible and the rigid body drives the system to instability, as shown in Figure 23.

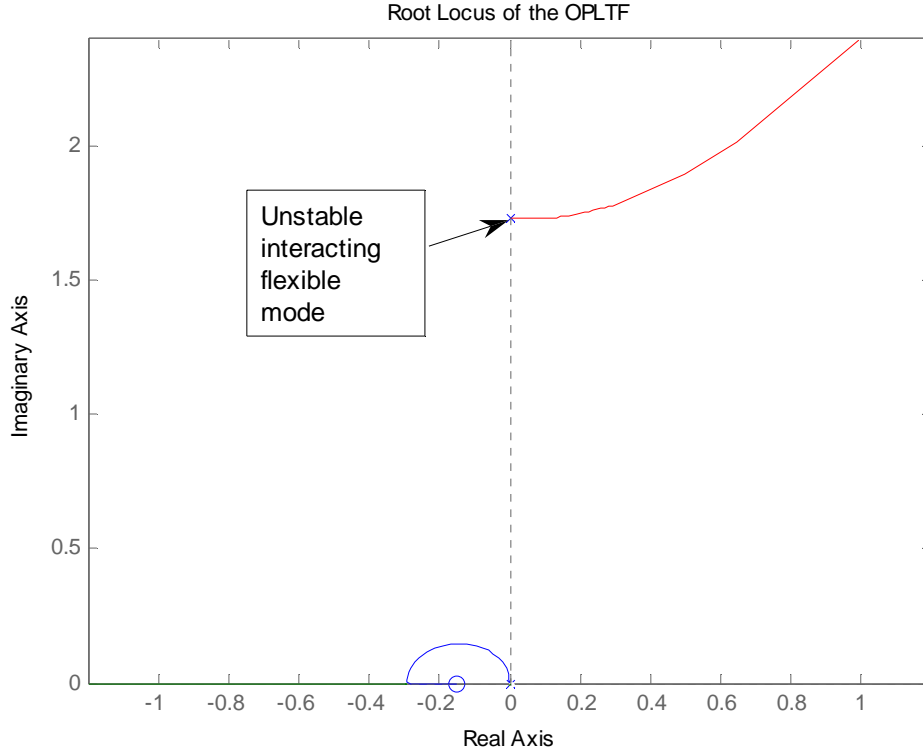


Figure 23. Root locus of the two mass system spring OPLTF.

In order to guarantee system's stability, a nonminimum-phase all-pass structure filter is applied to provide a phase shift at the flexible body frequency. The basic characteristics of this filter are the system's gain conservation and the flexibility mode's phase delay. For the purpose of this analysis, the coefficients of this filter are set as:

$$\omega_z = \omega_p = \sqrt{2K} \text{ and } \zeta_p = -\zeta_z = 0.5$$

In Figure 24, we show the Bode plot of the nonminimum-phase all-pass filter, which presents an amplitude of 0 dB and a phase change from  $360^\circ$  to  $0^\circ$ . The factor  $\zeta_p$  assigns the slope of the phase plot, meaning that bigger  $\zeta_p$  corresponds to a smoother slope. [Wie].

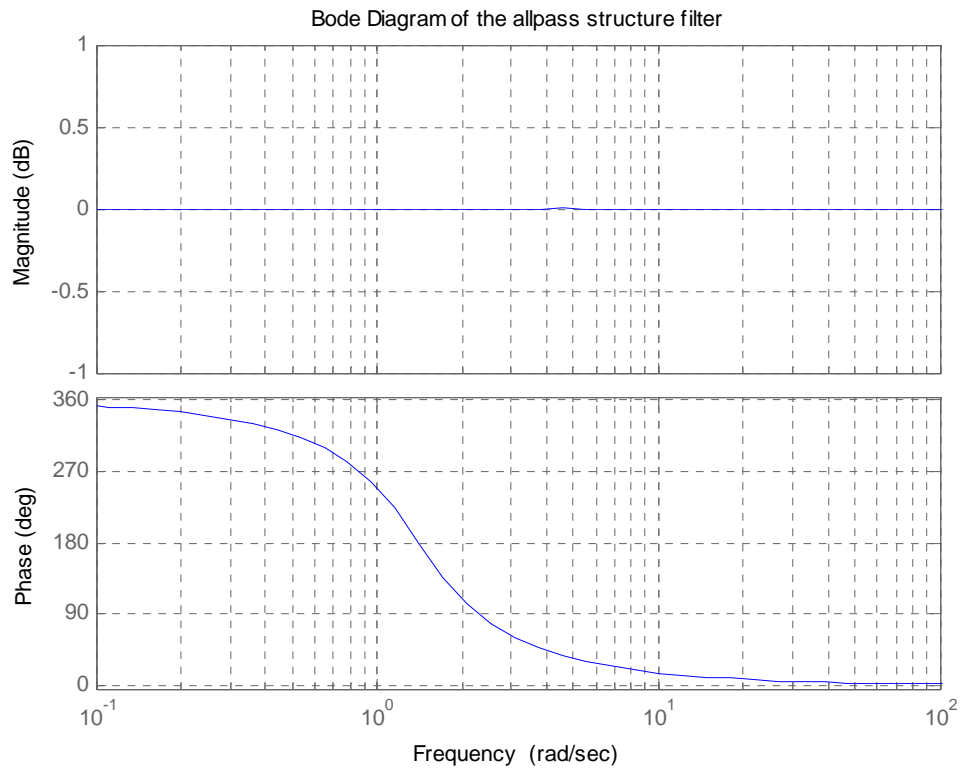


Figure 24. Bode plot of the all-pass nonminimum phase structure filter.

When we include the all-pass structural filter in the control, the system becomes stable with a PM of  $37.75^\circ$  and a GM of 1.86 dB, as indicated in Figure 25.

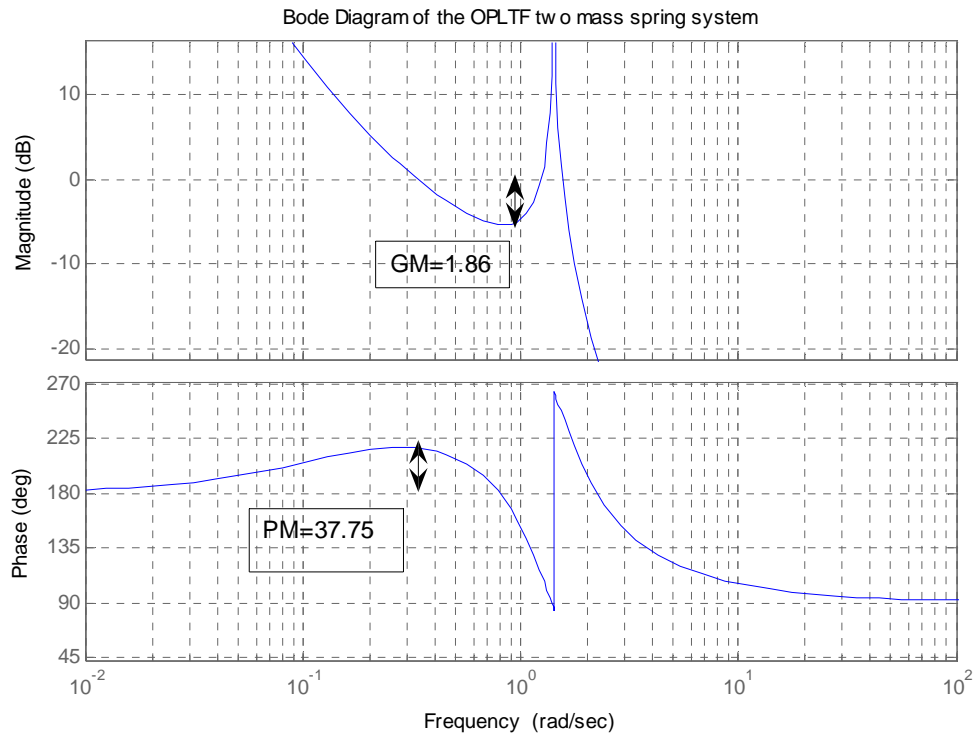


Figure 25. Bode plot of the OPLTF of the two-mass-spring system.

As a consequence, the impulse response of the CLTF, illustrated in Figure 26, shows rapidly decaying oscillations.

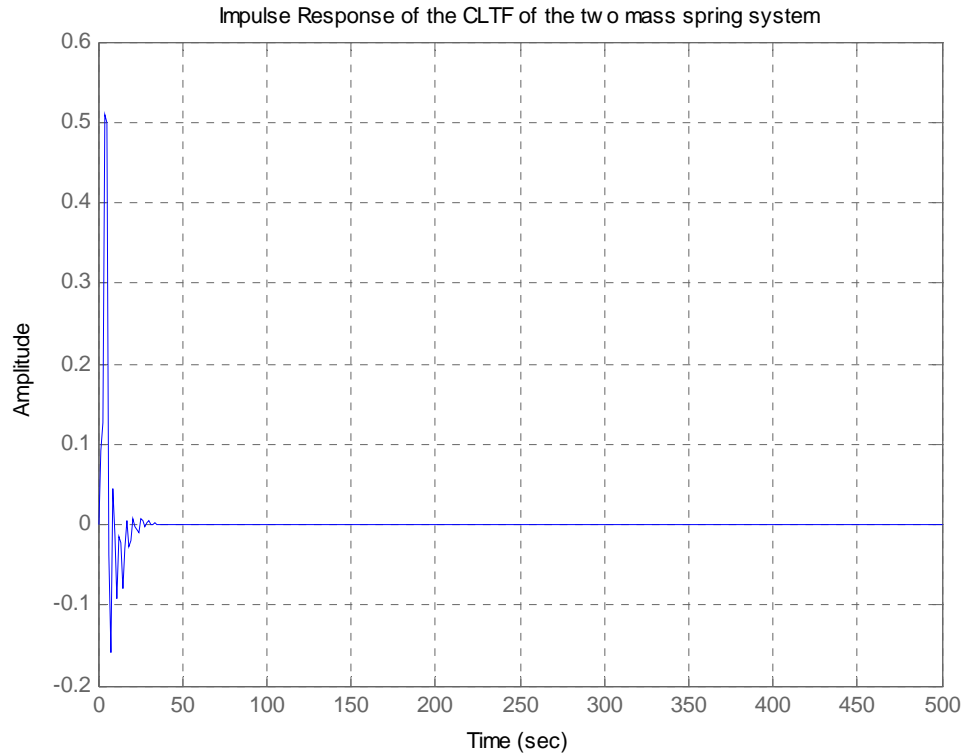


Figure 26. Impulse response of the CLTF of the two-mass-spring system.

## B. COMPARISON OF THE LQG/LTR AND NONMINIMUM PHASE NOTCH FILTER DESIGNS

Continuing the study of this model, an LQG/LTR controller is designed as it was done in Chapter III. The system appears to have better stability margins for different values of factor  $g$ , as indicated in Table 4.

<b>Performance of the LQG / LTR controller for the two-mass-spring model</b>				
<b>Increment in the scalar g</b>	<b>1</b>	<b>10</b>	<b>100</b>	<b>1000</b>
<b>PM (degrees)</b>	<b>46.9541</b>	<b>52.5630</b>	<b>59.6880</b>	<b>63.5380</b>
<b>GM (dB)</b>	<b>3.8842</b>	<b>3.1796</b>	<b>5.3836</b>	<b>10.041</b>
<b>Gain Cross Over frequency (Hz)</b>	<b>0.8709</b>	<b>0.9454</b>	<b>3.1718</b>	<b>6.1809</b>
<b>Phase Cross Over frequency (Hz)</b>	<b>0.2130</b>	<b>0.2900</b>	<b>1.5550</b>	<b>1.5846</b>

Table 4. Performance of the LQG/LTR controller for the two-mass spring model.

However, the nonminimum-phase all-pass structure filter seems to be more robust than the LQG/LTR controller. Indeed, as the flexibility mode frequency is increased, the system is driven to instability, as indicated in Figure 27.

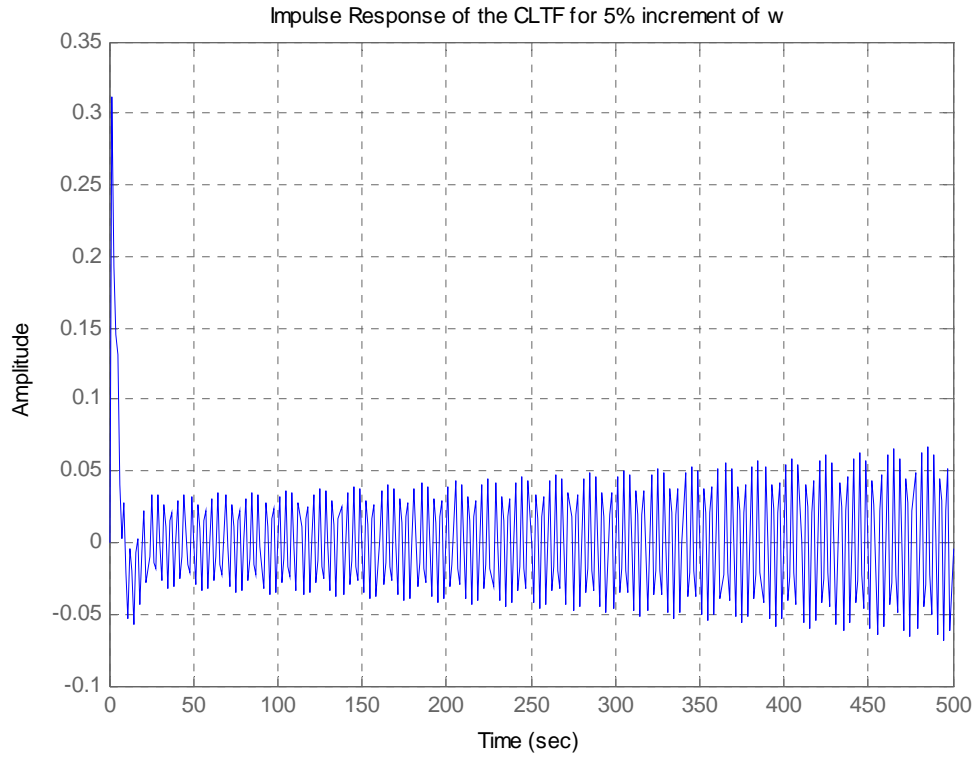


Figure 27. Impulse response of the CLTF of the two-mass spring system for 5% increment of the flexibility mode frequency with LQG/LTR.

On the other hand, the notch filter meets the target of the optimal control, and this is indicated in Table 5, where the reader can see the stability margins as the flexibility mode frequency increases.

<b>Notch Filter performance</b>			
<b>Increment in the flexibility mode frequency</b>	<b>10%</b>	<b>20%</b>	<b>30%</b>
<b>PM (degrees)</b>	<b>38.5373</b>	<b>34.4075</b>	<b>21.9943</b>
<b>GM (dB)</b>	<b>2.4401</b>	<b>3.0701</b>	<b>3.7549</b>
<b>Gain Cross Over frequency (Hz)</b>	<b>0.7989</b>	<b>0.7989</b>	<b>0.7989</b>
<b>Phase Cross Over frequency (Hz)</b>	<b>0.2781</b>	<b>1.7893</b>	<b>1.9183</b>

Table 5. Notch filter performance for the two-mass spring system.

In Figure 28, we show the Nyquist plots of the OPLTF of the nonminimum-phase structural filter design within 0 to 30 percent increment of the nominal frequency. It can be seen that none of the plots crosses the -1 point, thus guaranteeing closed loop stability. However, the stability margins of the OPLTF are becoming smaller as the frequency of the flexible mode is increased.

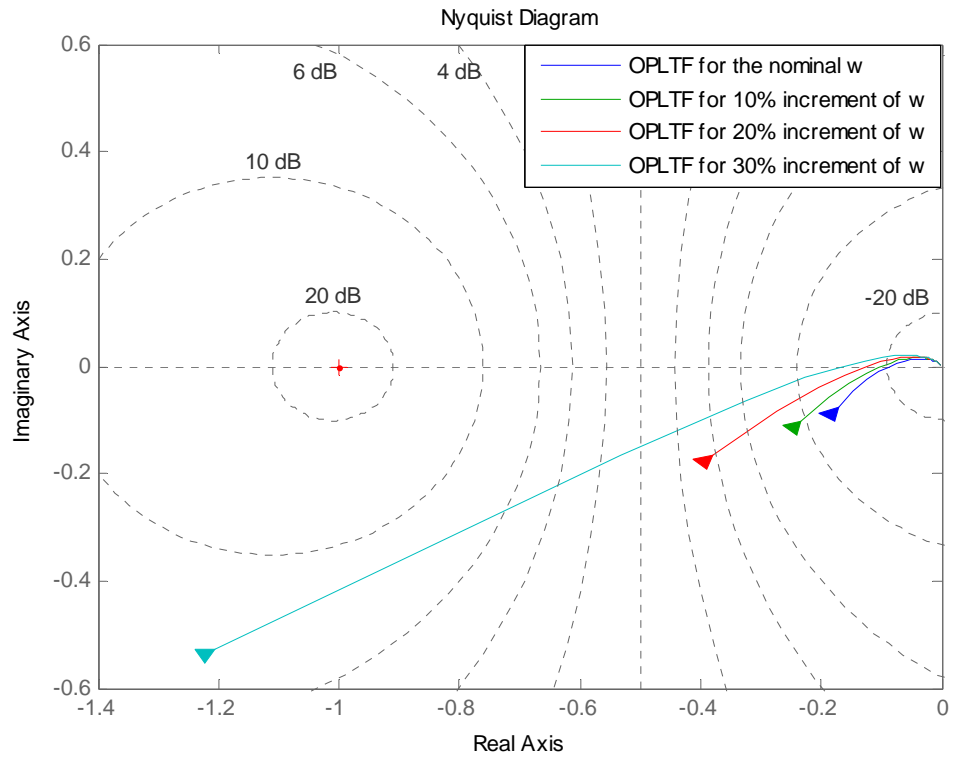


Figure 28. Nyquist plots of the Notch filter system OPLTF for several values of the flexibility mode frequency.

## VI. CONCLUSIONS AND RECOMMENDATIONS

The main goal at this thesis is to develop an algorithm to reject perturbations caused by flexible modes in a control system. The main characteristic of the flexible mode is the existence of pairs of conjugate poles and zeros on the imaginary axis. LQR and LQG design, in conjunction with the LTR method, and, finally, an application of an all-pass structural filter at the feedback loop of the control system were used to guarantee the stability and the robustness of the system.

As expected, the LQR design ensures satisfactory stability while requiring knowledge of the feedback states. On the other hand, the LQG design is more realistic since it uses states estimated by a Kalman-Bucy filter. Of course, the control system loses its previous stability margins and it becomes less robust to uncertainties in the knowledge of frequencies. By using the LTR method, we can recover part of the LQR stability margins. We have shown that as we increase the noise covariance matrix at the input of the system, the efficiency of the filter becomes poorer but the overall system became more robust. Results showed that the model could retain the closed loop stability in the presence of 10% increment of the flexible mode frequency.

In the last chapter we addressed the concept of an all-pass nonminimum phase second-order structural filter and we studied its performance for a specific example. In particular, we designed an LQG/LTR controller for this example and we compared the results of these two approaches. We showed that the structural filter design is more robust than the LQG/LTR. More specifically, the structural filter design maintained the stability margins in desirable levels as the flexible mode frequency increased up to 30% in contrast to the LQG/LTR controller that became unstable in up to a 5% increment.

In this thesis, we presented a different but an effective way of using the classical methods in rejecting the perturbations of flexible modes in a control system. Nonminimum phase structural filters can be very effective for stabilizing a control system if the designer understands how the system's zero-pole pairs are interacting with each other and chooses the appropriate location on the RHP to place the zeros of the filter.

Furthermore, the research in this thesis is performed in conjunction with the thesis of K. Tzello [Tzello]. The latter investigates the estimation of the flexible modes frequencies which can be used in the proposed controller in an adaptive implementation.

In this thesis we concentrated our effort on a fixed gain system for control of flexible structures. The fixed gains can be periodically updated using estimates of the frequencies of the structure. A more advanced implementation would be a fully adaptive approach, where the gains of the controller are updated directly from output measurements. This would lead to an adaptive controller, available in the literature. Questions on convergence and robustness in actual applications will have to be addressed.

## LIST OF REFERENCES

- [Astrom] Astrom, K. and B. Wittenmark. *Computer-Controlled Systems: Theory and Design*, 3rd edition, Prentice-Hall Inc., Upper Saddle River, NJ, 1997.
- [Savant] Savant, S. and S. Hostetter. *Design of Feedback Control Systems*, 3rd edition, Saunders College Publishing, 1994.
- [Preumont] Preumont, A. *Vibration Control of Active Structures*, 2nd edition Kluwer Academic Publishers, 1996.
- [Hespanha] Hespanha, Joao P. Undergraduate Lecture Notes on LQG/LQR Controller, <http://www.ece.ucsb.edu/~hespanha/ece147c/web/lqrlqgnotes.pdf>, April 16, 2007.
- [Wie] Wie, Bong and Kuk Whan Byun. "A New Concept of Generalized Structural Filtering for Active Vibration Control Synthesis," AIAA-1987-2456 IN: AIAA Guidance, Navigation and Control Conference, Monterey, CA, August 17-19, 1987, Technical Papers Volume 2 (A87-50401 22-08). New York, American Institute of Aeronautics and Astronautics, 1987, pp. 919-929.
- [Tzellos] Tzellos, Konstantinos. "Filter Bank Approach to the Estimation of Flexible Modes in Dynamics Systems," MSEE Thesis, Naval Postgraduate School, Monterey, CA, June 2007.

THIS PAGE INTENTIONALLY LEFT BLANK

## INITIAL DISTRIBUTION LIST

1. Defense Technical Information Center  
Ft. Belvoir, Virginia
2. Dudley Knox Library  
Naval Postgraduate School  
Monterey, California
3. Chairman, Code EC  
Department of Electrical and Computer Engineering  
Naval Postgraduate School  
Monterey, California
4. Roberto Cristi  
Department of Electrical and Computer Engineering  
Naval Postgraduate School  
Monterey, California
5. Xiaoping Yun  
Department of Electrical and Computer Engineering  
Naval Postgraduate School  
Monterey, California
6. Carlos Borges  
Department of Applied Mathematics  
Naval Postgraduate School  
Monterey, California
7. Manos Eleftherios  
Hellenic Navy  
Athens, Greece